P H Y S I C A L   R E V I E W   L E T T E R S

Spin Echo of a Single Electron Spin in a Quantum Dot

F. H. L. Koppens, K. C. Nowack, and L. M. K. Vandersypen

Kavli Institute of NanoScience Delft, P.O. Box 5046, 2600 GA Delft, The Netherlands
(Received 3 November 2007; published 10 June 2008)

We report a measurement of the spin-echo decay of a single electron spin confined in a semiconductor quantum dot. When we tip the spin in the transverse plane via a magnetic field burst, it dephases in 37 ns due to the Larmor precession around a random effective field from the nuclear spins in the host material. We reverse this dephasing to a large extent via a spin-echo pulse, and find a spin-echo decay time of about 0.5 μs at 70 mT. These results are in the range of theoretical predictions of the electron spin coherence time governed by the electron-nuclear dynamics.

Isolated electron spins in a semiconductor can have very long coherence times, which permits studies of their fundamental quantum mechanical behavior, and holds promise for quantum information processing applications [1,2]. For ensembles of isolated spins, however, the slow intrinsic decoherence is usually obscured by a much faster systematic dephasing due to inhomogeneous broadening [3,4]. The actual coherence time must then be estimated using a spin-echo pulse that reverses the fast dephasing [5,6].

For a single isolated spin there is no inhomogeneous broadening due to averaging over a spatial ensemble. Instead, temporal averaging is needed in order to collect sufficient statistics to characterize the spin dynamics. In some cases, this averaging can also lead to fast apparent dephasing that can be (largely) reversed using a spin-echo technique. This is possible when the dominant influence on the electron spin coherence fluctuates slowly compared to the electron spin dynamics, but fast compared to the required averaging time. Such a situation is common for an electron spin in a GaAs quantum dot where the hyperfine interaction with the nuclear spins gives rise to a slowly fluctuating nuclear field, resulting in a dephasing time of tens of nanoseconds [7–11]. The effect of the low-frequency components of the nuclear field can be reversed to a large extent by a spin-echo technique. For two-electron spin states, this was demonstrated by rapid control over the exchange interaction between the spins [11]. The application of a spin-echo technique on a single electron spin is required when using the spin as a qubit. Furthermore, erasing the fast dephasing allows for a more detailed study of the remaining decoherence processes, including those caused by the electron-nuclear spin dynamics [12–18].

Here, we report the use of a spin-echo technique for probing the coherence of a single electron spin confined in an electrostatically defined GaAs quantum dot [shown in Fig. 1(a)]. We find that the spin-echo decay time $T_{2,\text{echo}}$ is about 0.5 μs, more than a factor of 10 longer than the dephasing time T_2^*, indicating that the echo pulse reverses the dephasing to a large extent. These findings are consistent with (extrapolations of) theoretical predictions for this system [15–17], as well as with earlier echo measurements

on two-electron spin states in a similar quantum dot system [11], and with mode locking measurements of single spins in an ensemble of self-assembled quantum dots [19].

The measurement scheme is depicted in Fig. 1(a) (similar as reported in [20]). Two quantum dots are tuned such that one electron always resides in the right dot and a second electron can flow through the two quantum dots only if the spins are antiparallel. For parallel spins, the second electron cannot enter the right dot due to the Pauli exclusion principle, and is blocked in the left dot [21]. This allows us to initialize the system in a mixed state of $|\uparrow\uparrow\rangle$ and $|\downarrow\downarrow\rangle$ (stage 1), although from now on we assume the initial state is $|\uparrow\uparrow\rangle$, without loss of generality. Next the electron spins are manipulated with a sequence of radio frequency (rf) bursts (stage 2), while a voltage pulse ΔV_p is applied to one of the gates so that the exchange interaction between the two spins is negligible and tunneling is prohibited
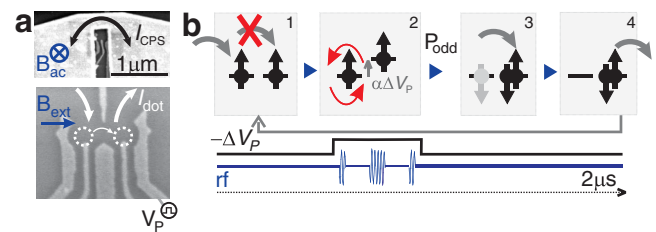

FIG. 1 (color online). (a) Bottom: Scanning electron microscope (SEM) image of the Ti/Au gates on top of a GaAs/AlGaAs heterostructure containing a two-dimensional electron gas 90 nm below the surface. White arrows indicate current flow through the two coupled dots. The gate labeled with V_p is connected to a homemade bias tee (rise time 150 ps) to allow fast pulsing of the dot levels. Top: SEM image of the on-chip coplanar strip line (CPS), separated from the surface gates by a 100-nm-thick dielectric. Because of the geometry of the strip line, the oscillating field with amplitude B_{ac} and frequency f_{ac} is generated primarily perpendicular to the static field B_{ext}, which is applied in the plane of the two-dimensional electron gas. (b) Schematic of the electron cycle (time axis not to scale). The voltage ΔV_p (with lever arm α) on the gate detunes the dot levels during the manipulation stage (applied bias over the dots is 1.5 mV).

regardless of the spin states. Once the pulse is removed, electron tunneling is allowed again, but only for antiparallel spins (stages 3 and 4). The entire cycle lasts 2 μs and is continuously repeated, resulting in a current flow which is proportional to the average probability P_{odd} to find antiparallel spins at the end of stage 2.

We first use this scheme to measure the dephasing of the spin via a Ramsey-style experiment [see pulse sequence in Fig. 2(a)]. After a $\pi/2$ pulse that creates a coherent superposition between $|\uparrow\rangle$ and $|\downarrow\rangle$, the spin is allowed to freely evolve for a delay time τ (for now, we reason just in a single-spin picture, see below and Ref. [20]).
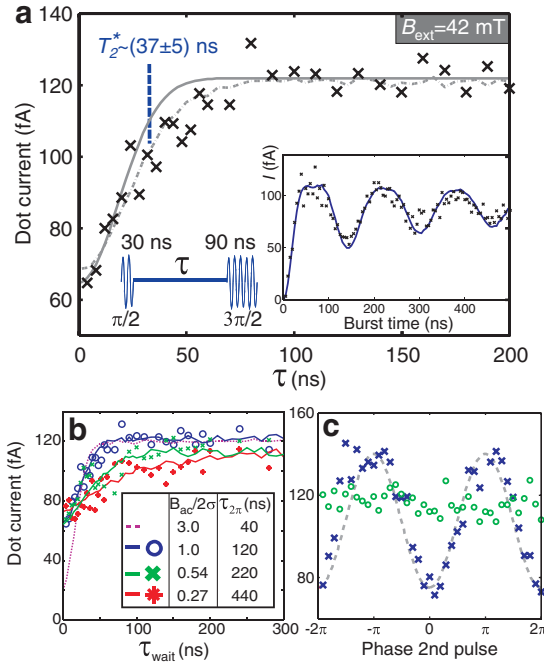

FIG. 2 (color online). (a) Ramsey signal as a function of free-evolution time τ (each point averaged over 20 s at constant $B_{\text{ext}} = 42$ mT, $f_{\text{ac}} = 210$ MHz, $B_{\text{ac}} = 3$ mT). As shown in the inset, this gives a Rabi period $\tau_{2\pi}$ of 120 ns [20]. In order to optimize the visibility of the decay, the second pulse is a $3\pi/2$ pulse instead of the usual $\pi/2$ pulse. Solid line: Gaussian decay with $T_2^* = 30$ ns, corresponding to $\sigma = 1.5$ mT. Dotted line: Numerically calculated current. First P_{odd} is computed taking $\sigma = 1.5$ mT, and then the current is derived as $I_{\text{dot}} = P_{\text{odd}}(m + 1)80 + 23$ fA (m and offset due to background current obtained from fit). A current of 80 fA corresponds to one electron transition per 2 μs cycle, and m is the additional number of electrons that tunnel through the dot on average before the current is blocked again. Here, we find $m = 1.44$; the deviation from the expected $m = 1$ is not understood and discussed in [20]. (b) Measured and numerically calculated Ramsey signal for a wide range of driving fields. We assume $\sigma = 1.5$ mT, and estimate the current as $P_{\text{odd}}(m + 1)80 + 23$ fA ($m = 1.5$) for $\tau_{2\pi} = 40$–220 ns, and as $P_{\text{odd}}(m + 1)80 + 43$ fA ($m = 1.5$) for $\tau_{2\pi} = 440$ ns. (c) Ramsey signal as a function of the relative phase between the two rf bursts for $\tau = 10$ (crosses) and 150 ns (circles). Gray dashed line is a best fit of a cosine to the data.

Subsequently, a $3\pi/2$ pulse is applied, with a variable phase. Ideally, if both rf pulses have the same phase (in the rotating frame), the spin is rotated back to $|\uparrow\rangle$, and the system returns to spin blockade. If the phases between the two pulses are 180°, the spin is rotated to $|\downarrow\rangle$, and the blockade is lifted. Figure 2(c) shows that for small τ, the signal indeed oscillates sinusoidally as a function of the relative phase between the two rf pulses, analogous to the well-known Ramsey interference fringes. For large τ, however, the spin completely dephases during the delay time, and the fringes disappear [Fig. 2(c)]. When the two pulses are applied with the same phase [Fig. 2(a)], we find that the signal saturates on a time scale of $T_2^* \sim 37$ ns (obtained from a Gaussian fit, see below), which gives a measure of the dephasing time.

The observed Ramsey decay time is the result of the hyperfine interaction between the electron spin and the (about 10^6) randomly oriented nuclear spins in the host material. The interaction can be described by a nuclear field with a spectral content ranging from milliseconds to seconds [22]. This is much longer than the 2 μs cycle time, but much shorter than the averaging time for each measurement point (~ 20 s). The nuclear field in the z direction $B_{N,z}$ modifies the Larmor precession frequency of the electron spin resulting in a coherence decay of $e^{-(\tau/T_2^*)^2}$, with $T_2^* = \sqrt{2}\hbar/g\mu_b\sigma \sim 30$ ns [7,8] (assuming $\sigma = 1.5$ mT, extracted from the Rabi oscillations, see [23]). This decay is plotted in Fig. 2(a) (solid line). However, the observed Ramsey signal cannot be compared directly with this curve because we have to take into account the effect of the nuclear field during the $\pi/2$ and $3\pi/2$ pulses as well. Essentially, $B_{N,z}$ shifts the electron spin resonance condition, and as a result the fixed-frequency rf pulses will be somewhat off resonance which decreases the fidelity of the rotations.

We include these effects in a simulation of the spin dynamics, and consider from here on not just a single spin but the actual two-spin system. We thereby leave out the exchange interaction, as it can be neglected during the manipulation stage. At the end of the cycle, the two-spin state is then given by $|\psi(\tau, B_{L,R})\rangle = U^L_{3\pi/2}(B_L)U^R_{3\pi/2}(B_R) \times V^L_\tau(B_L)V^R_\tau(B_R)U^L_{\pi/2}(B_L)U^R_{\pi/2}(B_R)|\uparrow\uparrow\rangle$. Here, $U^{L,R}_\theta(B_{L,R})$ is the single-spin time-evolution operator (for an intended θ rotation) resulting from the driving field and the z component of the nuclear fields in the left and right dot, B_L and B_R. The operator $V^{L,R}_\tau(B_{L,R})$ represents the single-spin evolution during a time τ in the presence of the nuclear field only. We can then compute P_{odd} at the end of the pulse sequence, averaging over two independent Gaussian distributions of nuclear fields in the left and right dot:

$$P_{\text{odd}}(\tau) = \frac{1}{2\pi\sigma^2} \iint e^{-[(B_L^2 + B_R^2)/2\sigma^2]}$$
$$\times \tilde{P}_{\text{odd}}(\tau, B_{L,R}) dB_L dB_R;$$
$$\tilde{P}_{\text{odd}}(\tau, B_{L,R}) = |\langle\psi(\tau, B_{L,R})|\uparrow\downarrow\rangle|^2 + |\langle\psi(\tau, B_{L,R})|\downarrow\uparrow\rangle|^2.$$

This numerically calculated $I_{dot} \propto P_{odd}(\tau)$ is plotted in Fig. 2(a) (dotted line). We see that the predicted decay time is longer when the rotations are imperfect due to resonance offsets. This is more clearly visible in Fig. 2(b), where the computed curves are shown together with Ramsey measurements for a wide range of driving fields. The experimentally observed Ramsey decay time is longer for smaller B_{ac}, in good agreement with the numerical result. This effect can be understood by considering that a burst does not (much) rotate a spin when the nuclear field pushes the resonance condition outside the Lorentzian line shape of the excitation with width B_{ac}. If the spin is not rotated into a superposition, it cannot dephase either. As a result, the cases when the nuclear field is larger than the excitation linewidth do not contribute to the measured coherence decay. The recorded dephasing time is thus artificially extended when low-power rf bursts are used ($B_{ac}/2\sigma \lesssim 1$). However, in Fig. 2(a), this is only a small effect.

We remark that the experiments discussed here allow us to probe single-spin coherence even though the experiments are carried out with two spins and the rf excitation is applied to both dots simultaneously. First, the two spins have different resonance conditions due to the nuclear fields which are generally different in the two dots. Second, the exchange interaction between the two spins can be neglected during the manipulation stage. Therefore, for small enough driving fields ($B_1 < \sigma$) the rf pulses rotate predominantly one spin (reported and analyzed in [20,23]), and the observed Ramsey and echo decay is expected to be due to single-spin decoherence.

We now test to what extent the electron spin dephasing is reversible using a spin-echo pulse. In Fig. 3(a) the applied pulse sequence (inset) and the measured signal as a function of the total free-evolution time (main panel) are shown. We see immediately that the spin-echo decay time $T_{2,echo}$ is much longer than the dephasing time T_2^*. This is also clear from the data in Fig. 3(c), which is taken in a similar fashion as the Ramsey data in Fig. 2(c), but now with an echo pulse applied halfway through the delay time. Whereas the fringes were fully suppressed for a 150 ns delay time without an echo pulse, they are still clearly visible after 150 ns if an echo pulse is used. As a further check, we measured the echo signal as a function of $\tau_1 - \tau_2$ [Fig. 3(b)]. As expected, the echo is optimal for $\tau_1 = \tau_2$ and deteriorates as $|\tau_1 - \tau_2|$ is increased. The dip in the data at $\tau_1 - \tau_2 = 0$ has a half width of ~ 27 ns, similar to the observed T_2^*.

Upon closer inspection, the spin-echo signal in Fig. 3(a) reveals two types of decay. First, there is an initial decay with a typical time scale of 33 ns (obtained from a Gaussian fit), which is comparable to the observed Ramsey decay time when using the same B_{ac}. This fast initial decay occurs because the echo pulse itself is also affected by the nuclear field. As a result it fails to reverse the electron spin time evolution for part of the nuclear spin
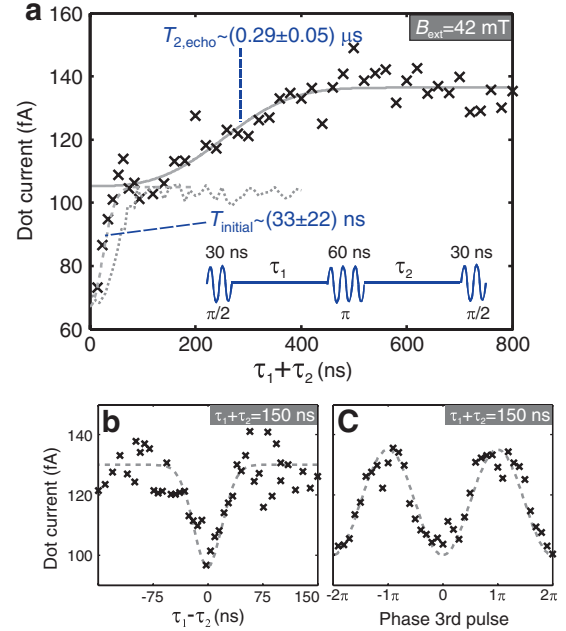

FIG. 3 (color online).   (a) Spin-echo signal as a function of total free-evolution time $\tau_1 + \tau_2$ (each point averaged over 20 s at constant $B_{ext} = 42$ mT, $f_{ac} = 210$ MHz, $B_{ac} = 3$ mT). Dashed line: Best fit of a Gaussian curve to the data in the range $\tau_1 + \tau_2 = 0$–100 ns. Solid line: Best fit of $e^{-[(\tau_1+\tau_2)/T_{2,echo}]^3}$ to the data in the range $\tau_1 + \tau_2 = 100$–800 ns. Dotted line: Numerically calculated dot current $P_{odd}(m + 1)80 + 25$ fA, taking $\sigma = 1.5$ mT in both dots and $m = 1.83$. The scatter in the data points is not due to the noise of the measurement electronics (noise floor about 5 fA), but is caused by incomplete averaging over the statistical nuclear field. (b) Spin-echo signal as a function of $\tau_1 - \tau_2$. Dashed line: Best fit of a Gaussian curve to the data. (c) Spin-echo signal for $\tau_1 + \tau_2 = 150$ ns as a function of the relative phase between the first two and third pulse. Dashed line is the best fit of a cosine to the data.

configurations, in which case the fast dephasing still occurs, similar as in the Ramsey decay. To confirm this, we calculate numerically the echo signal, including the effect of resonance offsets from the nuclear fields, similar as in the simulations of the Ramsey experiment. We find reasonable agreement of the data with the numerical curve [dotted line in Fig. 3(a)], regarding both the decay time and the amplitude.

The slower decay in Fig. 3(a) corresponds to the loss of coherence that cannot be reversed by a perfect echo pulse. We extract the spin-echo coherence time $T_{2,echo}$ from a best fit of $a + be^{-[(\tau_1+\tau_2)/T_{2,echo}]^d}$ to the data (a, b, $T_{2,echo}$ are fit parameters and d is kept fixed) and find $T_{2,echo} = (290 \pm 50)$ ns at $B_{ext} = 42$ mT for $d = 3$ [see Fig. 3(a), solid line]. We note that the precise functional form of the decay is hard to extract from the data, but we find similar decay times and reasonable fits for the range $d = 2$–4.

Measurements at higher B_{ext} are shown in Figs. 4(a) and 4(b). Here, experiments were only possible by decreasing the driving field and, as expected, we thus find a longer initial decay time, similar as seen in Fig. 2(b) for Ramsey
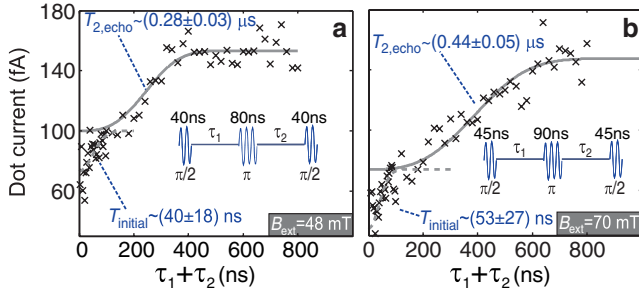
FIG. 4 (color online).   (a) Spin-echo signal at $B_{\rm ext} = 48$ mT ($f_{\rm ac} = 280$ MHz) and (b) 70 mT ($f_{\rm ac} = 380$ MHz). Pulse sequence depicted in the insets. Solid lines and dashed lines are best fits to the data as in Fig. 3(a).

measurements. The longer decay time from which we extract $T_{2,\rm echo}$ tends to increase with field, up to 0.44 μs at $B_{\rm ext} = 70$ mT. This is roughly in line with the spin-echo decay time of 1.2 μs observed for two-electron spin states at $B_{\rm ext} = 100$ mT [11].

We now examine what mechanism limits $T_{2,\rm echo}$. The z component of the nuclear field can change due to the spin-conserving flip-flop terms $H_{\rm ff} = \frac{1}{2}(S_+ h_- + S_- h_+)$ in the hyperfine Hamiltonian $\mathbf{S} \cdot \mathbf{h}$, and due to the dipole-dipole interaction between neighboring nuclear spins. Because of the large energy mismatch (at the applied magnetic fields) between the electron and nuclear spin Zeeman splitting, only the energy-conserving higher-order contributions from $H_{\rm ff}$ can lead to flip-flop processes between two non-neighboring nuclear spins mediated by virtual flip-flops with the electron spin [13–16,18]. It is predicted that this hyperfine-mediated nuclear spin dynamics can lead to a field dependent free-evolution decay of about 1–100 μs for the field range 1–10 T [15,16,18]. Interestingly, some theoretical studies [14,16] have predicted that this type of nuclear dynamics is reversible (at sufficiently high field) by an echo pulse applied to the electron spin. The coherence decay time due to the second possible decoherence source, namely the dipole-dipole interaction, is theoretically predicted to be 10–100 μs [16,17], independent of magnetic field (once $B_{\rm ext} > 0.1$ mT, the dipole field of one nucleus seen by its neighbor).

Decoherence mechanisms other than the interaction with the nuclear spin bath must also be considered. One possibility is spin exchange with electrons in the reservoir via higher-order tunneling processes. However, we expect that the typical time scale of this process is very long because (during the manipulation stage) the energy required for one of the electrons to be promoted to a reservoir (>100 μeV) is much larger than the tunnel rate (<0.1 μeV). In principle, the exchange coupling between the spins in the two quantum dots could spoil the spin-echo effect, but we estimate this coupling to be much smaller than $1/T_{2,\rm echo}$. Altogether, the most likely limitation to the observed $T_{2,\rm echo}$ is hyperfine-mediated flip-flops between any two nuclear spins.

To conclude, we have performed time-resolved measurements of the dephasing of a single electron spin in a quantum dot caused by the interaction with a quasistatic nuclear spin bath. We have largely reversed this dephasing which occurs in ~30 ns by the application of a spin-echo technique and find a $T_{2,\rm echo}$ of 0.29 and 0.44 μs at magnetic fields of 42 and 70 mT, respectively. While even longer coherence times are expected at higher magnetic fields and multiple pulse sequences [24,25], the observed decay times are already sufficiently long for further exploration of electron spins in quantum dots as qubit systems.

[1] D. Loss and D. P. DiVincenzo, Phys. Rev. A **57**, 120 (1998).
[2] R. Hanson, *et al.*, Rev. Mod. Phys. **79**, 1217 (2007).
[3] M. V. G. Dutt, *et al.*, Phys. Rev. Lett. **94**, 227403 (2005).
[4] A. S. Bracker, *et al.*, Phys. Rev. Lett. **94**, 047402 (2005).
[5] B. Herzog and E. L. Hahn, Phys. Rev. **103**, 148 (1956).
[6] J. P. Gordon and K. D. Bowers, Phys. Rev. Lett. **1**, 368 (1958).
[7] A. V. Khaetskii, D. Loss, and L. Glazman, Phys. Rev. Lett. **88**, 186802 (2002).
[8] I. A. Merkulov, A. L. Efros, and M. Rosen, Phys. Rev. B **65**, 205309 (2002).
[9] A. C. Johnson, *et al.*, Nature (London) **435**, 925 (2005).
[10] F. H. L. Koppens, *et al.*, Science **309**, 1346 (2005).
[11] J. R. Petta, *et al.*, Science **309**, 2180 (2005).
[12] R. de Sousa and S. Das Sarma, Phys. Rev. B **68**, 115322 (2003).
[13] W. A. Coish and D. Loss, Phys. Rev. B **70**, 195340 (2004).
[14] N. Shenvi, R. de Sousa, and K. B. Whaley, Phys. Rev. B **71**, 224411 (2005).
[15] C. Deng and X. Hu, Phys. Rev. B **73**, 241303(R) (2006).
[16] W. Yao, R. B. Liu, and L. J. Sham, Phys. Rev. B **74**, 195301 (2006).
[17] W. M. Witzel and S. Das Sarma, Phys. Rev. B **74**, 035322 (2006).
[18] W. Coish, J. Fischer, and D. Loss, arXiv:0706.0180.
[19] A. Greilich, *et al.*, Science **313**, 341 (2006).
[20] F. H. L. Koppens, *et al.*, Nature (London) **442**, 766 (2006).
[21] Normally, all three triplet states can block current flow. However, due to the difference of nuclear fields in the two dots, one of the triplets T_0 is admixed with the singlet S, which lifts the blockade [10].
[22] D. J. Reilly, *et al.*, arXiv:0712.4033.
[23] F. H. L. Koppens, *et al.*, Phys. Rev. Lett. **99**, 106803 (2007).
[24] W. M. Witzel and S. Das Sarma, Phys. Rev. Lett. **98**, 077601 (2007).
[25] W. Yao, R. B. Liu, and L. J. Sham, Phys. Rev. Lett. **98**, 077602 (2007).